Saudi Journal of Biological Sciences 27 (2020) 3169–3179

Contents lists available at ScienceDirect

Saudi Journal of Biological Sciences

journal homepage: www.sciencedirect.com

Original article

Remote sensing of 10 years changes in the vegetation cover of the northwestern coastal land of Red Sea, Saudi Arabia

Awad Alharthi [a], Mohamed A. El-Sheikh [a,b,*], Mohamed Elhag [c], Abdulrahman A. Alatar [a], Ghanim A. Abbadi [d], Eslam M. Abdel-Salam [a], Ibrahim A. Arif [a], Ariej A. Baeshen [e], Ebrahem M. Eid [f,1]

[a] Botany & Microbiology Department, College of Science, King Saud University, P.O. Box. 2455, Riyadh 11451, Saudi Arabia
[b] Botany Department, Faculty of Science, Damanhour University, Damanhour, Egypt
[c] Department of Hydrology and Water Resources Management, Faculty of Meteorology, Environment & Arid Land Agriculture, King Abdulaziz University, Jeddah 21589, Saudi Arabia
[d] Department of Biological Sciences, Faculty of Science, Kuwait University, P.O. Box 5969, Safat 13060, Kuwait
[e] Biological Sciences Department, Faculty of Science, University of Jeddah, Saudi Arabia
[f] Biology Department, College of Science, King Khalid University, Abha 61321, P.O. Box 9004, Saudi Arabia

ARTICLE INFO

Article history:
Received 10 June 2020
Revised 3 July 2020
Accepted 15 July 2020
Available online 23 July 2020

Keywords:
Accuracy assessment
Land use/land cover
Support vector machine
Thematic change detections

ABSTRACT

Accurate and up to date land use and land cover (LU/LC) changes information is the main source to understanding and assessing the environmental outcomes of such changes and is important for development plans. Thus, this study quantified the outlines of land cover variation of 10-years in the northwestern costal land of the Red Sea, Saudi Arabia. Two different supervised classification algorithms are visualized and evaluated to preparing a policy recommendation for the proper improvements towards better determining the tendency and the proportion of the vegetation cover changes. Firstly, to determine present vegetation structure of study area, 78 stands with a size of 50 × 50 m were analysed. Secondly, to obtain the vegetation dynamics in this area, two satellite images of temporal data sets were used; therefore, SPOT-5 images were obtained in 2004 and 2013. For each data set, four SPOT-5 scenes were placed into approximately 250-km intervals to cover the northwestern coastal land of the Red Sea. Both supervised and non-supervised cataloguing methods were attained towards organise the study area in 4-major land cover classes through using 5 various organizations algorithms. Approximately 900 points were evenly distributed within each SPOT-5 image and used for assessment accuracy. The floristic composition exhibits high diversity with 142 species and seven vegetation types were identified after multivariate analysis (VG I: *Acacia tortilis-Acacia ehrenbergiana*, VG II: *Acacia tortilis-Stipagrostis plumosa,* VG III: *Zygophyllum coccineum-Zygophyllum simplex*, VG IV: *Acacia raddiana-Lycium shawii-Anabasis setifera*, VG V: *Tamarix aucheriana-Juncus rigidus*, VG VI: *Capparis decidua-Zygophyllum simplex* and VG VII: *Avicennia marina-Aristida adscensionis*) and ranged between halophytic vegetation on the coast to xerophytic vegetation with scattered *Acacia* trees inland. The dynamic results showed rapid, imbalanced variations arises between 3-land cover classes (areas as urban, vegetation and desert). However, these findings shall serve as the baseline data for the design of rehabilitation programs that conserve biodiversity in arid regions and form treasured resources for an urban planner and decision makers to device bearable usage of land and environmental planning.

1. Introduction

Distribution and structure of vegetations are major components in the function of coastal ecosystems that offer numerous important ecosystem services in many regions of the globe (Arshad et al., 2018). In the recent years of Saudi Arabia at the Red Sea, the costal vegetation degradation has been increased in the last years. The current vegetation is affected by the increasing aridity due to climate change and anthropogenic factors such as urbanization (El-Sheikh et al., 2019). The consideration in present trend of

* Corresponding author at: Botany & Microbiology Department, College of Science, King Saud University, P.O. Box. 2455, Riyadh 11451, Saudi Arabia.
E-mail address: melsheikh@ksu.edu.sa (M.A. El-Sheikh).
[1] Permanent address: Botany Department, Faculty of Science, Kafr El-Sheikh University, Kafr El-Sheikh 33516, Egypt.
Peer review under responsibility of King Saud University.

Production and hosting by Elsevier

https://doi.org/10.1016/j.sjbs.2020.07.021
1319-562X/

vegetation alterations will leads to the potential necessity of sustainable management of natural habitats in the costal lands. In addition to the increasing aridity, the urbanization in Saudi Arabia represents a major land type of land transformation, which has been regarded as one of most important challenges for the conservation of natural vegetation lands from urban lands (El-Sheikh et al., 2019). The applications of change detection and the monitoring of land-use/ land-cover (LU/LC) varies and applied in multiple fields associated with (i) land degradation and also desertification (Adamo and Crews-Meyer, 2006; Gao and Liu, 2010) (ii) urban-sprawl (Shalaby and Tateishi, 2007), (iii) urban landscape of outlined changes (Dewan and Yamaguchi, 2008; Batisani and Yarnal, 2009; Elhag et al., 2013).

The common practice of remote sensing data analyses are anomaly detection, quantification and the mapping of LU/LC patterns and changes due to its availability and high degree of accuracy (Lu et al., 2004; Chen et al., 2005; Geymen and Baz, 2008; Abd El-Kawy et al., 2011). Numerous techniques have been accomplished for change detection which have been formulated, applied and estimated. The common principle method for the detection of LU/LC change is to compare two or more successive imageries covering the same area at different dates of acquisition (Lu et al., 2004). The detection of change is basically employing one of two basic methods (i) pixel-to-pixel comparison and (ii) post-classification comparison (PCC) (Lu et al., 2004). The PCC method is the highly accurate used for altering detection technique which identifies LC "land cover" changes through independently comparing the classification maps from different dates (Singh, 1989; Yuan et al., 1998). Temporal data are independently classified; therefore, direct comparability does not require any further adjustment (Singh, 1989; Coppin et al., 2004; Rivera, 2005; Zhou et al., 2008; Green, 2011). The PCC method has an additional advantage of indicating the nature of changes thematically (Mas, 1999; Yuan et al., 2005).

The exact and updated LU/LC variation data is required for understanding and evaluating the environmental consequences of specific changes (Giri et al., 2005) and is tremendously important for any kind of sustainable development program in which LU/LC serves as one of the important input criteria (Abd El-Kawy et al., 2011). Moreover, analysis and mapping over for both the current LU/LC situations and the changes in LU/LC over time is considered a major to better understand and provides solutions for specific problems such as economic, environment and social issues (Lu et al., 2004; Pelorosso et al., 2009). The valuation of the magnitude and pattern of different land cover types is a necessity for projecting the future of vegetation cover and land development, especially when the major land cover in the study area is rainwater dependent natural vegetation (Jensen et al., 1995). The remote sensing data is in the form of satellite images, in conjunction with Geographic information system (GIS), which has been widely applied and recognized as a powerful tool in detecting land cover changes (Jensen et al., 1995; Lu et al., 2004; Chen et al., 2005; Geymen and Baz, 2008; Wang and Xu, 2010).

In general, the current study enumerated the LU/LC patterns of the last decade in northwestern coastal region of Red Sea. The objectives are set primarily to evaluate and visualize couple of various supervised classification algorithms and to supply the recommended policies for an accurate enhancement towards better determining the tendency and the proportion of vegetation cover changes. This current study results would be relevant globally due to the extrapolated to comparable ecosystems in another planets. Moreover, the findings of the present study form valuable resources for an urban planners and decision makers to devise sustainable usage of land and environment planning for designing of rehabilitation programs that converse biodiversity in arid regions.

2. Materials and methods

2.1. Study area

The study area extends from Jeddah (N 21°46′41.4″ E 39°08′36.8″) to Haql (N 29°16′39.5″ E 34°56′17.8″) covering a distance of roughly 1174 km along the Hijaz mountains which located on the Arabian shield and encompass the mountain range at the northwestern part of Saudi Arabia, stretching out along the Red Sea cost. At the east, the mountain range is bordered through the Tihamah i.e., coastal region, which consists majorly of sand plains with varying soil depths and salts concentration. This area was selected because of its high importance in biodiversity conservation resulted from the presence of different unique habitats (coastal wetted habitats, sandy plains, inland desert, alluvial wadis networks, and rocky foothills) and plant species.

2.2. Data sampling of current vegetation

Seventy-eight stands with a size of 50 × 50 m at the coastal area from Jeddah to Haql (~1174 km) were selected at spring of 2014 to represent all habitat variations and analyse the vegetation structure of the study area. In each stand, species were listed and identified according to Chaudhary (1999–2001), and their life forms were classified. The plant cover value of all species in each stand was estimated as abundance cover % according to Kent (2012). To obtain the vegetation groups; the two-way indicator species analysis (TWINSPAN) and the detrended correspondence analysis (DECORANA) programs (Hill, 1979a,b) of multivariate analysis was applied on the matrix data-set (78 stands × 142 species cover values).

2.3. Field survey for vegetation cover changes

The current study area was surveyed with the aim of mapping the existing natural vegetation cover changes. Two transects were laid out: one between the Hijaz Mountains and the coast and one at the eastern side of the Hijaz Mountains. The western transect was laid out along the Saudi Arabian highway 5 between Jeddah and Haql. The eastern transect followed highway 15 and highway 328, starting between Makkah and Medina and ending before Al-Ula. The stand locations were chosen to cover most of the apparent variation in vegetation and habitat (Elhag and Bahrawi, 2014a,b). Stands were selected through subjective judgement. The upper sectors of the mountains represent a translational zone between the monsoon and Mediterranean climates, which is influenced by the proximity to the Red Sea and the mountain range (Abd El-Ghani, 1997). In the lowlands, the climate is dry, with rainfall not exceeding 100 mm each year. This leads to the lowlands generally having more scarce vegetation, except for wadis, which have traditionally represented a richer ecosystem than the surrounding desert plains (Kassas and Imam, 1954).

2.4. Dataset

Two temporal sets of SPOT-5 images were acquired in 2004 and 2013. Each dataset was comprised of four consequent images of Saudi Arabia's west coast from Haql north to Jeddah south (Fig. 1).

2.5. Image classification process

In a SPOT satellite image, the spectral brightness of each picture elements (pixel) is recorded in four (SPOT-5) different wavelength bands. A pixel is characterized by its spectral signature, which is determined by the relative reflectance in the different wavelength

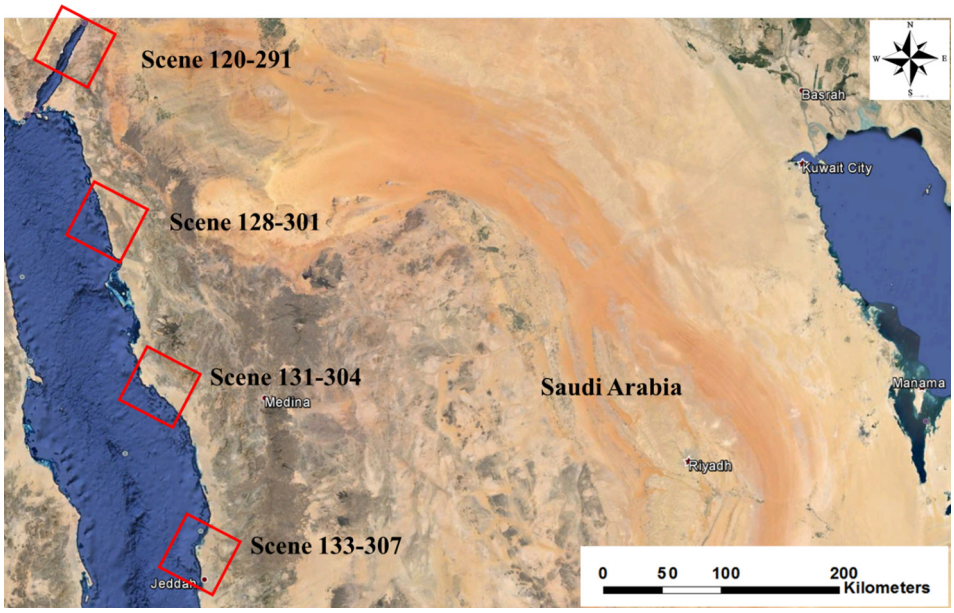

Fig. 1. Study area locations highlighted in red.

bands. Multispectral classification is an information extraction process that analyses the spectral signatures and then separates pixels into categories based on similar signatures (Briem et al., 2002). Image classification has become an important part in the fields of remote sensing, image analysis, and pattern recognition (Kloer, 1994; Richards and Richards, 1999).

2.6. Classification methods

Generally, there are two classification methods: the unsupervised classification and the supervised. Unsupervised classification proceeds with only minimal interaction with the analyst. On the other hand, supervised classification procedures require considerable interaction with the analyst, who must guide the classification by identifying small regions on the image that are known to belong to each category.

2.6.1. Unsupervised classification

Unsupervised classification is a computer-implemented process through which each measurement vector is assigned to a class according to a specified decision rule, where in contrast with supervised classification, the possible classes have been defined based on inherent data characteristics rather than on training samples (Swain and Davis, 1981). Based on the calculation of the Optimum Index Factor (OIF), the algorithm used to compute OIF for any subset of channels follows Chavez et al. (1982):

$$OIF = \frac{\sum_{k=1} s_k}{\sum_{j=1} Abs_{(r_j)}} \tag{1}$$

where

s_k is the standard deviation from channel k, and r_j is the absolute value of the correlation coefficient between any of the two channels being evaluated.

2.6.2. Supervised classification

Supervised classification is a computer-implemented process through which each measurement vector is assigned to a class according to a specified decision rule, where the possible class have been defined based on representative training samples of known identity (Swain and Davis, 1981). The first step in the supervised classification is to select training sites for each of the terrain categories. Two different supervised classification algorithms are used in the current research study, namely, Maximum Likelihood - ML and Support Vector Machine - SVM. Maximum Likelihood classification is performed according to the following equation:

$$g_i(x) = 1np(\omega_i) - 1/21n\left|\sum i\right| - 1/2(x - m_i)^T \sum_{i}^{-1} (x - \mu_i) \tag{2}$$

where

i is class; x is n-dimensional data (where n is the number of bands); $p(\omega i)$ is the probability that class ωi occurs in the image and is assumed the same for all classes; $|\Sigma i|$ is the determinant of the covariance matrix of the data in class ωi; $\Sigma i\text{-}1$ is its inverse matrix; and mi is mean vector.

Support Vector Machine is performed according to the following equation:

$$K(x_i, x_j) = \tanh(gx_i^T x_j + r) \tag{3}$$

where

g is the gamma term in the kernel function for all kernel types except linear, and r is the bias term in the kernel function for the polynomial and sigmoid kernels.

2.7. Classification accuracy assessment

A total number of 900 points of ground truth data were collected from January to March 2014, and the points encompass the major land use/land cover in the study area. The points were evenly distributed along the study area (225 points per scene). The points were converted into 50 m^2 polygons under the GIS environment for accessibility reasons. Validation points were individually assigned to four different land cover categories: sea, mountain, desert and vegetation. The points were used to calculate user's, producer's and overall accuracies. The producer's accuracy is calculated as follows:

$$\text{Producer accuracy} = \frac{C_{aa}}{C_{*a}} \times 100\% \quad (4)$$

where

C_{aa} is the element at position a^{th} row and a^{th} column, and C_{*a} is the column sum.

The user's accuracy is calculated as follows:

$$\text{User accuracy} = \frac{C_{ii}}{C_{i*}} \times 100\% \quad (5)$$

where

C_{ii} is the element at position a^{th} row and a^{th} column, and C_{i*} is the row sum.

Overall accuracy is calculated as follows:

$$\text{User accuracy} = \frac{\sum_{a=1}^{U} C_{aa}}{Q} \times 100\% \quad (6)$$

where

Q and U are the total number of pixels and classes, respectively. Matching of the user's and producer's accuracies delivers precision to the classification and assures a robust liability of the implemented accuracy assessment (Cohen, 1960; Congalton, 1991). K_{hat} statistics is a second measure accuracy agreement. This measure of agreement is based Congalton and Mead (1983) findings. K_{hat} was calculated using the following equation:

$$K_{hat} = \frac{N \cdot \sum_{i=1}^{r} x_{ii} - \sum_{i=1}^{r} (x_{ij} \cdot x_{ji})}{N^2 - \sum_{i=1}^{r} (x_{ij} \cdot x_{ji})} \quad (7)$$

where

r is the number of rows in the error matrix; x_{ii} is the number of observations in row i and column i (the diagonal cells); x_{ij} is the total observations of row i; x_{ji} is the total observations of column i; and N is the total of observations in the matrix.

2.8. Post-classification comparison

Post-classification comparison takes places after classifying the rectified images separately from two time periods (2004 and 2013) following Mas (1999) and Coppin et al. (2004). Each date of imagery was satisfactorily classified, and then compared and analysed to conduct and change the detection according to Lu et al. (2004) and Huang et al. (2008). Fig. 2 shows the steps of post-classification in the study area.

3. Results and discussion

The floristic composition contains 142 species from 41 families; Fabaceae had the highest percentage (12.5%), followed by Chenopodiaceae (10.2%) and Poaceae (9.2%). The maximum percentage of life-form was characterized by 44% in perennial herbs (or sub-shrubs), followed through 27% in shrubs, 23% in -therophytes, and 6% of trees in the total flora (Appendix 1). The prevalence of therophytes is typically the main characteristic feature of arid regions, which are related with unpredictable rainfall, and the dominance of woody sub-shrubs is typical of wetted coastal habitat (Mahmoud et al., 1982; Abbadi and El-Sheikh, 2002; Al-Rowaily et al., 2012). Seven plant communities have been

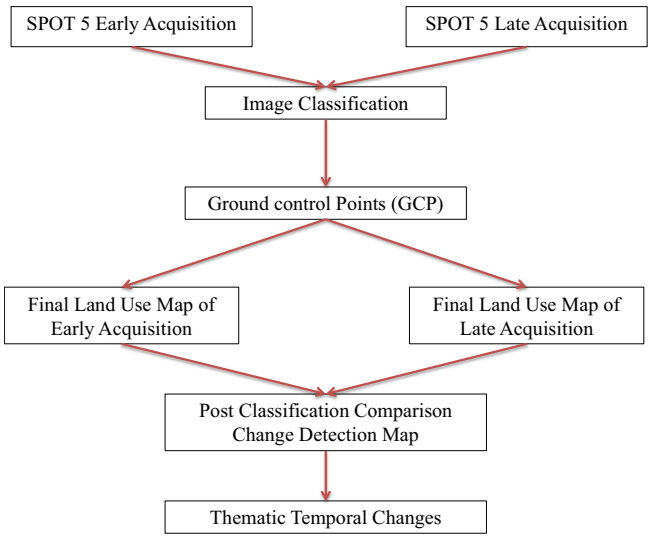

Fig. 2. Thematic change detection workflow.

documented after the application of TWINSPAN and DCA techniques (Fig. 3a, b); confirms as these communities are diverse species assemblages. VG I: *Acacia tortilis-Acacia ehrenbergiana* and VG II: *Acacia tortilis-Stipagrostis plumosa* are characterized by the presence of trees and grasses which inhabited the inland desert, sandy plains, alluvial wadis networks and rocky foothills of the Red Sea coastal area. On the other hand, the coastal wetted habitats are inhabited by halophytic communities, e.g., VG III: *Zygophyllum coccineum-Zygophyllum simplex*, VG IV: *Acacia raddiana-Lycium shawii-Anabasis setifera*, VG V: *Tamarix aucheriana-Juncus rigidus* and VG VI: *Capparis decidua-Zygophyllum simplex*. The VG VII: *Avicennia marina-Aristida adscensionis* occurred along the muddy banks of the Red Sea coast. The presence of most of these plant communities is more or less comparable to the previous studies on the study area (Vesey-Fitzgerald, 1957; Mahmoud et al., 1982). Therefore, the vegetation type of this area ranges between halophytic vegetation on the coast to xerophytic with scattered *Acacia* trees inland. In an arid-provinces, the changes in the vegetation composition are determined through the environmental factors and the human impacts as habitat shifting by the construction and modernization which induces heterogenicity concluded in space and time (Whitford, 2002; Jiao et al., 2011; Al-Rowaily et al., 2012).

Numerous algorithm classifications were implemented in supervised classification. Based on the Optimum Index Factor: OIF, unsupervised classification has promoted four various groups of Land Cover: LCs'. The statistical and graphical analysis of featured collections were implemented. The visible and infrared bands were involved in investigation apart from thermal infrared band. The summary in Table 1 indicates the cataloguing results in terms of both accuracy and Kappa statistics of each classification algorithm. Kappa statistics and overall accuracy promotes the Support Vector Machine over Maximum Likelihood classification, which agrees with Elhag et al. (2013). The error matrix was then performed to measure the user and producer's accuracies of the Support Vector Machine classification results as shown in Table 2 and 3 respectively.

In general, the output of algorithm classification in both accuracies and kappa statistics were amplified gradually from SPOT-5; early acquisition of 2004 to SPOT-5 late acquisition of 2013. The Maximum Likelihood classifier accuracies also increased towards the late acquisition of 2013. This could be explained because of an acquisition date of the second data-set (SPOT-5, 2013) are moderately close towards the collection date of the training and valida-

a) TWINSPAN:

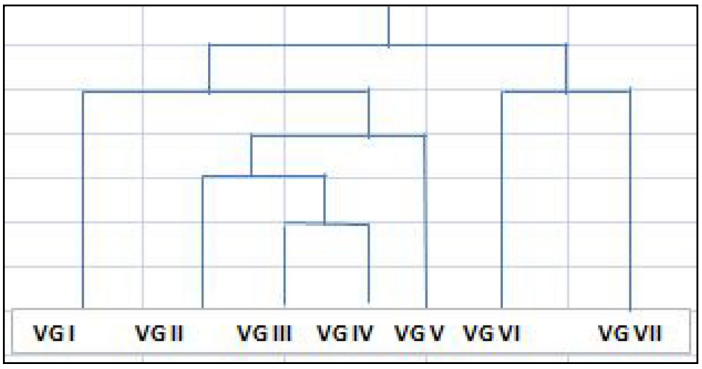

b) DCA:

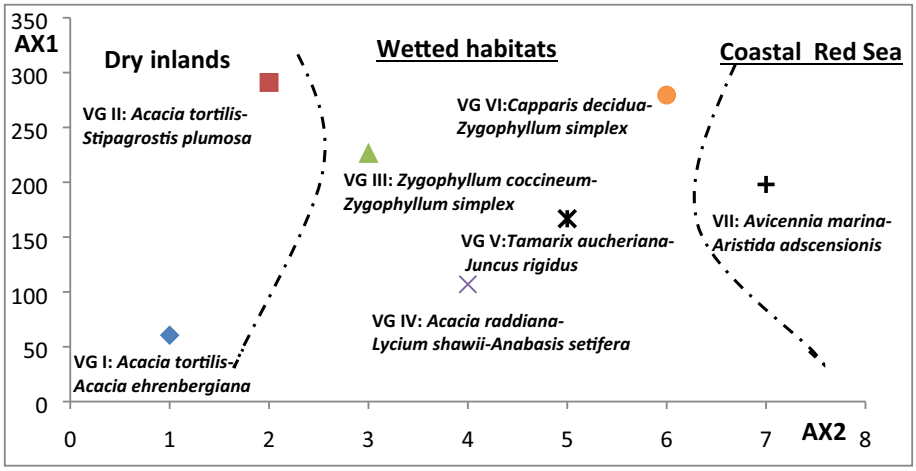

Fig. 3. Relationship between the seven plant communities after the application of TWINSPAN (a) and DCA (b).

Table 1
Overall accuracies and Kappa statistics of each classification algorithm.

Year of acquisition	SPOT 5, 2004		SPOT 5, 2013	
Classification algorithm	Overall	Kappa	Overall	Kappa
Maximum Likelihood	80.5%	0.75	93.5%	0.91
Support Vector Machine	90.3%	0.87	97.8%	0.97

Table 2
Error matrix for 2004 SPOT-5 Support Vector Machine (SVM) classification.

Item	Sea	Mountain	Desert	Vegetation	Sum	User's Accuracy
Sea	208	0	2	1	211	98.2%
Mountain	3	204	69	11	287	82.3%
Desert	7	95	216	15	333	77.8%
Vegetation	1	11	8	145	165	85.1%
Sum	219	310	295	172		
Producer's Accuracy	97.7%	57.5%	82.9%	88.4%	Overall Accuracy	90.3%

Table 3
Error matrix for 2013 SPOT-5 Support Vector Machine (SVM) classification.

Item	Sea	Mountain	Desert	Vegetation	Sum	User's Accuracy
Sea	124	0	13	0	137	98.3%
Mountain	0	139	45	5	189	78.1%
Desert	5	84	326	13	428	80.4%
Vegetation	3	18	21	124	166	78.9%
Sum	132	241	405	142		
Producer's Accuracy	98.1%	65.3%	84.6%	90.5%	Overall Accuracy	97.8%

tion points, which were also proved as an adequacy of the Support Vector Machine classifier over the rest of the classifier in the complex areas (Hsu et al., 2003; Batisani and Yarnal, 2009).

Fig. 4 showed each data set with respect to its classification and usage of map in SVM as the supervised classification algorithms. Four classes for LU/LC were detected in each temporal dataset.

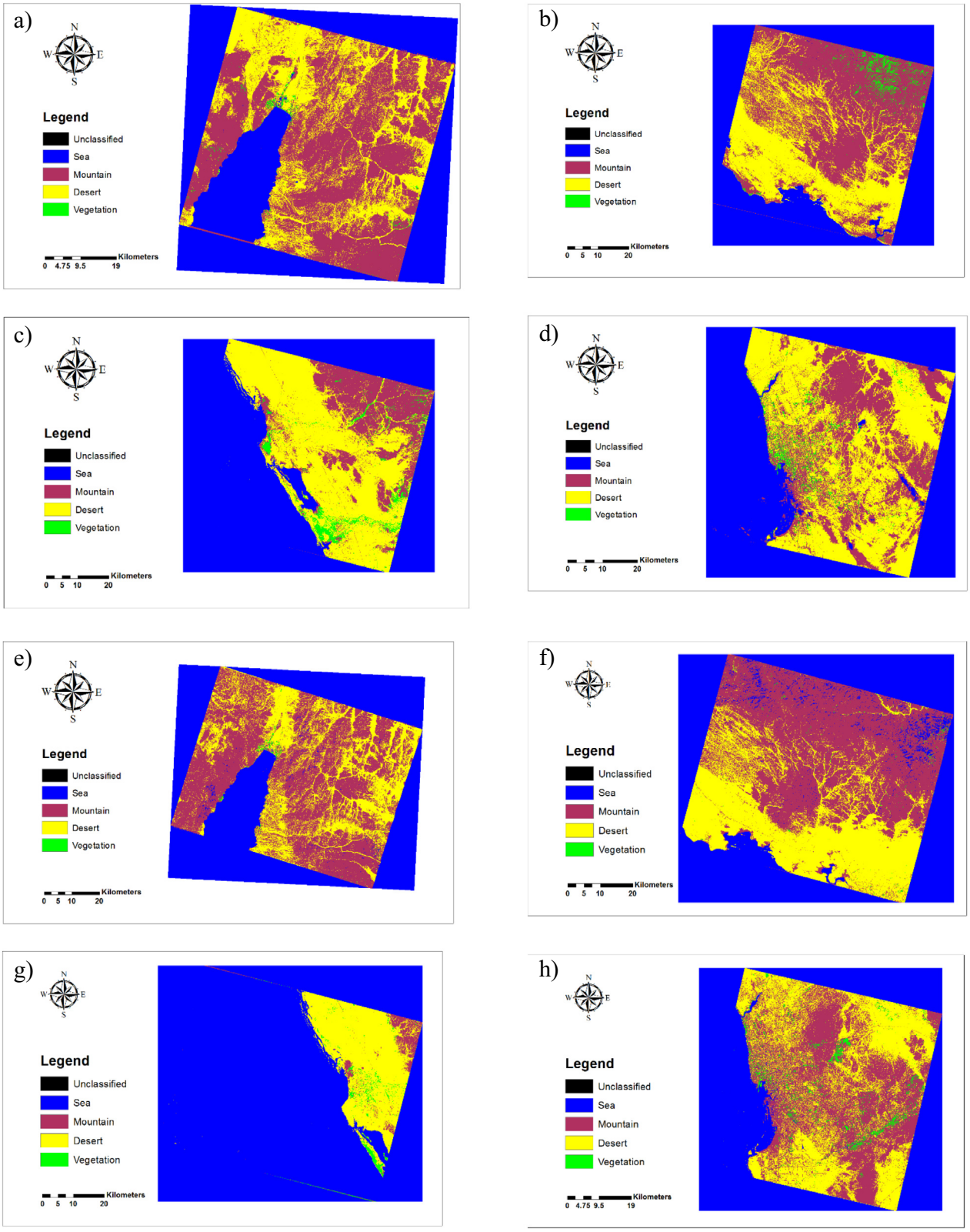

Fig. 4. Support Vector Machine (SVM) classification maps of SPOT 5 (a) early acquisition scene 120–291, (b) early acquisition scene 128–301, (c) early acquisition scene 131–304, (d) early acquisition scene 133–307, (e) late acquisition scene 120–291, (f) late acquisition scene 128–301, (g) late acquisition scene 131–304, and (h) late acquisition scene 133–307.

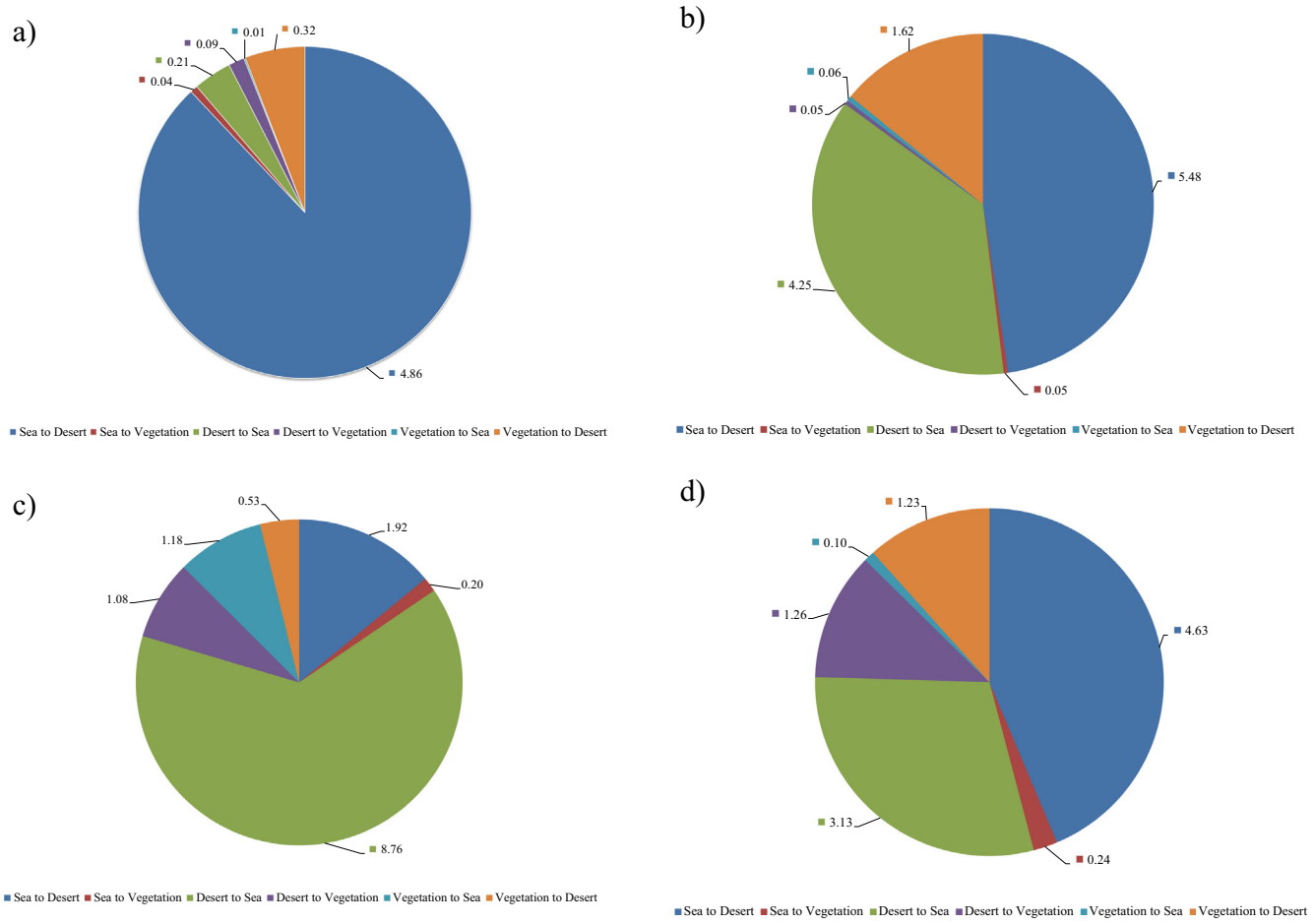

Fig. 5. (a) Temporal changes in scene 120–291, (b) scene 128–301, (c) scene 131–304, and (d) scene 133–307.

The composition for LU/LC was varied from scene to scene based on the scene morphological features (Elhag et al., 2013). The majority of LU/LC changes exist mainly along the coast indicating that the coastal ecosystem in those regions is highly fragile (Kumar et al., 2010). Sea water intrusion was the keystone LU/LC change detected in scene 131–304. The loss of vegetation was the main finding of temporal change detection subjected to scene 133–307. Urban expansion is the driving force for the loss of the natural vegetation in the study area (Elhag et al., 2013).

Fig. 5 quantifies the temporal changes in the present study. Fig. 5a shows that the majority of LU/LC changes were confined to sea sedimentation deposits (4.86%). Fig. 5b expressed two contradictory processes, sea water intrusion (4.25%) and sedimentation deposits (5.48%). Sea water intrusion was also the major temporal LU/LC changes in Fig. 5c counted for 8.76% of the changes. Fig. 5c demonstrated heterogeneity in the LU/LC temporal changes with major changes in the sea sedimentation deposits (4.63%) and minor changes in the degradation of coastal mangrove forests (0.10%).

Concerning temporal changes in vegetation cover confirmed in Fig. 6, the net vegetation cover changes were varied from one study site to another. In scene 120–291, vegetation loss was three times more than the vegetation gain, which requires immediate and intensive restoration plans. Similarly, the vegetation loss in scene 128–301 showed that the gain in vegetation cover is negligible compared to vegetation loss. Fig. 6b demonstrated that the bulk of the vegetation cover is mostly lost. Regulation procedures were to be adopted in both scene 131–304 and scene 133–307, where the loss of the vegetation cover was nearly equal to the vegetation gain. Regulation procedures are to maintain the existing vegetation cover and to restore degraded ones (Kumar et al., 2010).

4. Conclusion

The study quantified the patterns of LU/LC changes over ten years in the northwestern coastal land of the Red Sea. The two different supervised classification algorithms are used in the post-classification comparison method. The Support Vector Machine classifier was adopted because it's higher classification accuracies. Four classes of LU/LC and LC was produced, and both the vegetation and sediments main classes have changed rapidly in the area of the costal land. The vegetation cover class has decreased almost 19% through the time from 2004 to 2013. Meanwhile, sediments have increased by the same value of percentage (12%), despite of the proportional area in each class. The desert class has decreased because human intervention. Sedimentation deposits are remarkably noticeable along the shoreline of the coastal area. Usage of both multi spectral and temporal images for remote sensing data

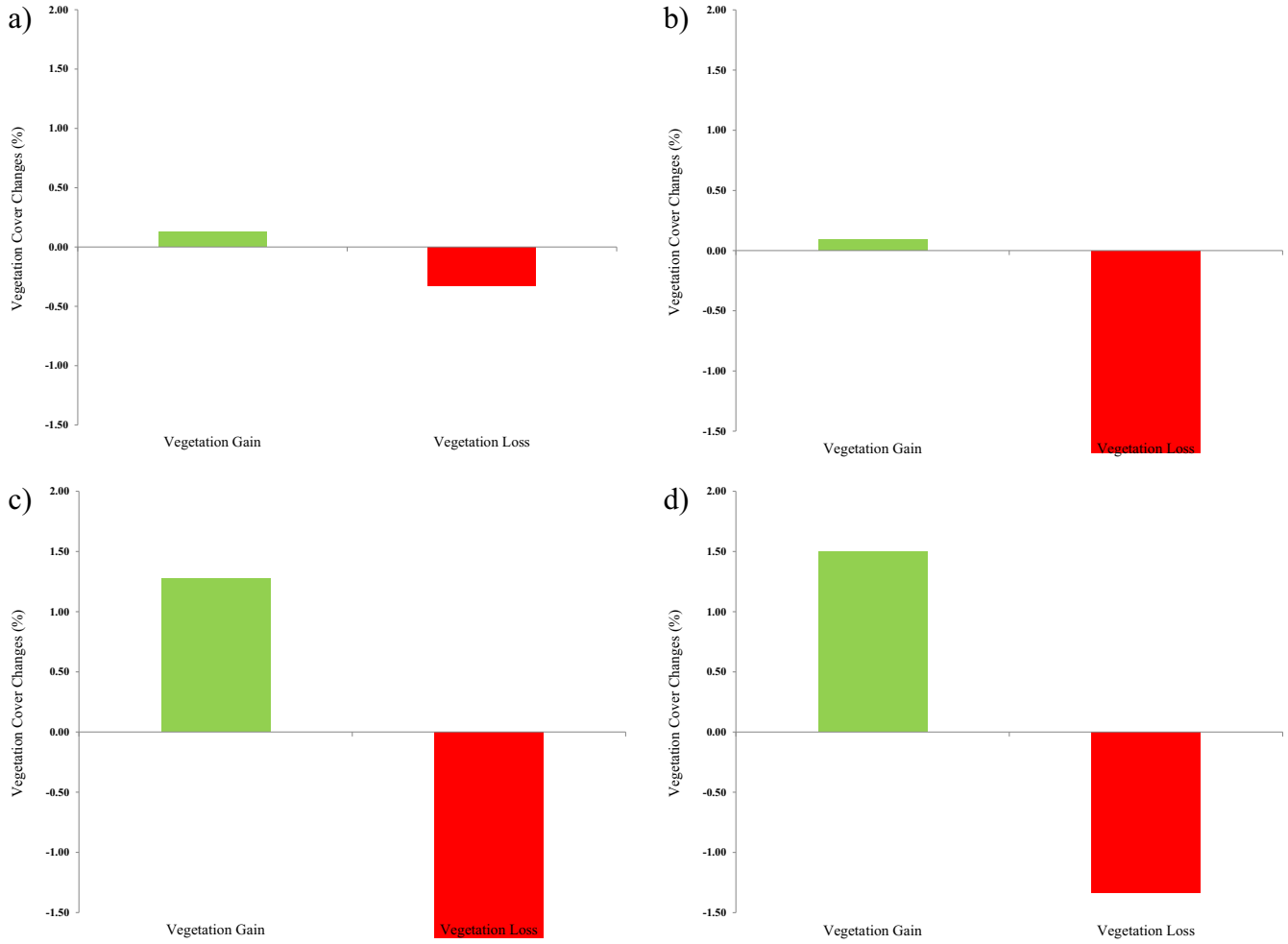

Fig. 6. Post-classification changes from (a) scene 120–291, (b) scene 128–301, (c) scene 131–304, and (d) scene 133–307.

provides the cost-effective tools to obtain valuable information for more efficient monitoring patterns of the developed land and further progress. The knowledge for GIS offers a flexible environment for storing, analysing and visualizing the digital data required for change assessing an improvement for database and also important for urban class investigation in further research. This could provide status of the vegetation cover land analysis, determine the definite restoration techniques that require be adopting, and setting the foundations for the planning policy intended to maximize and sustain of natural resources management. At last, the current study results strongly recommend new strategies for considering into account of the adjacent regions which may or may not be as direct or indirect affect the costal land development in the Saudi Arabia. For example, extension of urban should be strongly prohibited towards vegetation cover land and depositing the sediments towards shoreline, which could be wisely opted for perusing the effective plan of the management. The current study should be relevant globally due to the extrapolated of similar ecosystems in other parts of planet. Moreover, the findings of the present study form valuable resources for urban-planners and decision markers to devise sustainable land use and environmental planning and for the design of rehabilitation programs that conserve biodiversity in arid regions.

Declaration of Competing Interest

The authors declare that they have no known competing financial interests or personal relationships that could have appeared to influence the work reported in this paper.

Acknowledgements

The authors extend their appreciation to the Deanship of Scientific Research at King Saud University for funding this work through research group no. (RGP-1438-053).

Appendix 1. Synoptic table of the percentage cover species of 7 vegetation groups: VGI = Acacia tortilis-Acacia ehrenbergiana; VGII = Acacia tortilis-Stipagrostis plumosa; VG III = Zygophyllum coccineum-Zygophyllum simplex, VG IV = Acacia raddiana-Lycium shawii-Anabasis setifera; VG V = Tamarix aucheriana-Juncus rigidus; VG VI = Capparis decidua-Zygophyllum simplex and VG VII = Avicennia marina-Aristida adscensionis. A. = Annual; P. Perennial; Am = American; Eu.Sib = Euro siberian; IT = Irano turanian; Pac = Pacific; Med = Mediterranean; Med-IT = Mediterranean-Irano turanian; SA = Saharo Arabian; SM = Somali masai; SH = Sahel; TR AF = Tropical African.

Vegetation Group No.	L. form	Chorotype	I	II	III	IV	V	VI	VII
No. of stands			2	3	39	12	11	2	9
Zygophyllum simplex	A. Herb	SH-SM	1.0	1.0	5.1	3.0	5.0	3.0	2.0
Zygophyllum coccineum	P. Herb	SA	12.0	2.0	5.4	8.6	9.7	1.0	15.0
Acacia tortilis	Shrub	SH-SM	30.0	30.0	24.3	16.1	1.0	.	.
Acacia ehrenbergiana	Shrub	SH-SM	10.0	.	19.2	15.0	.	10.0	20.0
Senna italica	P. Herb	SH-SM	.	.	2.4	3.5	.	.	.
Haloxylon salicornicum	Shrub	SH-SM	.	3.0	3.4	3.0	6.0	.	.
Citrullus colocynthis	P. Herb	SA	.	.	1.0	1.0	.	.	.
Calotropis procera	Shrub	SH-SM	.	.	2.4	.	2.0	1.0	1.0
Chrozophora oblongifolia	P. Herb	IT	.	.	2.7	1.0	.	.	.
Anastatitica heirochuntica	A. Herb	SA	.	.	4.3	1.0	.	.	.
Suaeda monoica	Shrub	SH-SM	.	.	6.0	.	2.0	.	15.0
Acacia raddiana	Tree	SH-SM	.	.	.	32.5	5.0	.	.
Fagonia bruguieri	P. Herb	SA	.	1.0	1.0	2.7	.	.	.
Blepharis ciliaris	A. Herb	SA-IT	.	1.0	2.0	2.3	.	.	.
Fagonia indica	P. Herb	SA	.	.	1.5	1.5	.	.	1.0
Panicum turgidum	P. Grass	SA-SM	.	.	2.7	1.3	.	1.0	.
Salvadora persica	Shrub	SH-SM	.	.	3.5	15.0	.	.	.
Cadaba glandulosa	Shrub	SH-SM	.	.	.	5.0	.	.	.
Acacia oerfota	Shrub	TR-AF	.	.	.	10.0	.	.	.
Stipagrostis plumosa	P. Grass	SA-IT	.	7.0	5.0	3.0	.	.	.
Anabasis setifera	P. Herb	SA	.	.	22.3	11.0	.	.	.
Abutilon pannosum	Shrub	TR	.	.	4.6	.	.	.	.
Astragalus fatmensis	A. Herb	TR-AF	.	.	2.0	.	.	1.0	2.0
Convolvulus pilosellifolius	P. Herb	IT	.	.	3.3	.	.	.	.
Tamarix nilotica	Tree	SA	.	.	9.0	2.0	.	.	.
Capparis decidua	Tree	SH-SM	.	2.0	4.0	4.0	.	4.0	.
Prosopis juliflora	Tree	AM	.	.	3.4	.	1.0	.	.
Rhazya stricta	Shrub	SA	.	.	2.3	2.0	.	.	.
Paspalidium desertorum	P. Grass	SH-SM	.	.	3.5	.	.	.	.
Sporobolus spicatus	P. Grass	TR-AF	.	.	5.0	2.0	.	.	.
Suaeda aegyptiaca	A. Herb	SA	.	.	1.5	1.0	.	.	.
Maerua crassifolia	Tree	SH-SM	.	.	3.0	.	.	.	.
Cressa cretica	P. Herb	Med-IT	.	.	3.0	.	.	.	.
Salsola lachnantha	Shrub	IT	.	.	2.0	.	.	.	.
Cenchrus ciliaris	P. Grass	SA	.	.	1.5	.	.	.	.
Leptadenia pyrotechnica	Shrub	SA-SM	.	.	1.0	1.0	.	.	.
Odontanthera radians	A. Herb	TR-Af	.	.	1.0	.	.	.	.
Suaeda vermiculata	Shrub	SA	.	.	15.0	.	.	.	.
Lasiurus hirsutus	P. Grass	SA-SM	.	.	15.0	.	.	.	.
Zygophyllum qatarense	P. Herb	SA	.	.	5.0	.	.	.	.
Indigofera oblongifolia	Shrub	SA-SM	.	.	15.0	.	.	.	.
Digera muricata	A. Herb	TR-Af	.	.	5.0	.	.	.	.
Heliotropium europeam	P. Herb	EU-SI-ME-IT	.	.	5.0	.	.	.	.
Solanum sepicula	P. Herb	SA-SM	.	.	5.0	.	.	.	.
Taverniaria spartea	Shrub	SA	.	.	4.0	.	16.0	.	.
Ochradenus baccatus	Shrub	TR-Af	.	.	8.0	1.0	2.0	.	.
Aeluropus lagopoides	P. Grass	SA-IT	.	.	15.0	.	15.0	.	20.0
Zygophyllum album	P. Herb	SA	.	.	3.5	2.0	3.3	.	.
Tamarix aucheriana	Tree	SA-SM	.	.	5.0	.	10.3	.	.
Nitraria retusa	Shrub	SA	.	.	4.5	.	8.5	.	15.0
Lycium shawii	Shrub	SA-SM	.	.	2.0	7.3	3.5	.	.
Limonium axillare	P. Herb	TR-Af	.	.	4.0	2.0	8.0	.	.
Juncus rigidus	Shrub	EUSI-MED-IT	.	.	15.0	.	13.5	.	.
Hyphaene thebaica	Tree	SH-SM	.	.	2.0	2.0	1.0	.	.
Seidlitzia rosmarinus	Shrub	SA	.	.	1.0	.	25.0	.	.
Avicennia marina	Tree	TR	.	.	4.3	2.0	2.0	.	15.7
Halopeplis perfoliata	Shrub	SA	.	.	5.0	.	6.0	.	2.0
Halocnemum strobilaceum	Shrub	SA-MED-IT	2.0	.	.	.	.	.	3.5
Arthrocnemum macrostachyum	Shrub	SA-MED-IT	2.0	.	.	.	15.0	.	2.0
Calligonum comosum	Shrub	SA-IT	.	.	.	.	7.0	.	
Euphorbia retusa	P. Herb	SA	.	.	.	1.0	.	.	.
Forsskaolea tenacissima	P. Herb	SA-SM	.	1.0	.	1.0	.	.	.
Asphodelus fistulosus	A. Herb	–	.	.	.	1.0	.	.	.
Pergularia tomentosa	Shrub	SH-SM	.	.	.	1.0	.	.	.
Pulicaria guestii	P. Herb	SA	.	.	1.0	1.0	1.0	.	.
Launaea capitata	A. Herb	SA	.	.	1.0	1.0	.	.	.
Fagonia mollis	P. Herb	SA	.	.	1.0	2.0	.	.	.
Iphiona scabra	P. Herb	SA	.	.	5.0	.	1.0	.	.
Zygophyllum fabago	Shrub	IT	.	.	1.0	.	1.5	.	.
Cocculus pendulus	Climber	SH-SM	.	.	5.0	.	2.0	.	.
Cymodocea rotundata	P. Herb	Indian-Pac	.	.	16.0	.	.	.	.
Cadaba farinosa	Shrub	TR-AF	.	.	.	3.0	.	.	.
Retama raetam	Shrub	SA	.	.	3.0	.	.	.	.
Farsetia stylosa	P. Herb	SA	.	.	.	1.0	.	.	.

(*continued on next page*)

Appendix 1 (*continued*)

Vegetation Group No.	L. form	Chorotype	I	II	III	IV	V	VI	VII
Launaea mucronata	A. Herb	SA	.	.	.	1.0	.	.	.
Aristida adscensionis	P. Grass	SA-MED-IT	.	.	.	1.0	.	.	20.0
Gypsophila capillaris	P. Herb	SA	.	.	.	1.0	.	.	.
Ephedra foliata	Shrub	SH-SM	.	.	.	1.0	.	.	.
Lavandula coronopifolia	P. Herb	SA-SM	.	.	.	1.0	.	.	.
Echinops erinaceus	P. Herb	IT	.	.	.	1.0	.	.	.
Aerva javanica	P. Herb	TR	.	.	.	1.0	.	.	.
Plicosepalus curviflorus	Climber	TR-AF	.	.	.	2.0	.	.	.
Salsola spinescens	Shrub	SH-SM	.	.	.	1.0	.	1.0	.
Cistanche phylepae	P. Herb	SA	.	.	1.0	.	.	.	.
Senna alexandrina	Shrub	SA-SM	.	.	1.0	.	.	.	.
Tribulus pentandrus	A. Herb	SH-SM	.	.	1.0	2.0	.	.	1.0
Trigonella hamosa	A. Herb	SH-SM	.	.	1.0	.	.	.	.
Morettia parviflora	P. Herb	SH-SM	.	.	1.0	.	.	.	.

Fifty two species are considered as rare and their cover represents ≤2%.

References

Abbadi, G.A., El-Sheikh, M.A., 2002. Vegetation analysis of Failaka Island (Kuwait). J. Arid Environ. 50, 153–165. https://doi.org/10.1006/jare.2001.0855.

Abd El-Ghani, M.M., 1997. Phenology of ten common plant species in western Saudi Arabia. J. Arid Environ. 35, 673–683. https://doi.org/10.1006/jare.1996.0193.

Abd El-Kawy, O.R., Rød, J.K., Ismail, H.A., Suliman, A.S., 2011. Land use and land cover change detection in the western Nile delta of Egypt using remote sensing data. Appl. Geogr. 31, 483–494. https://doi.org/10.1016/j.apgeog.2010.10.012.

Adamo, S.B., Crews-Meyer, K.A., 2006. Aridity and desertification: Exploring environmental hazards in Jáchal,Argentina. Appl. Geogr. 26, 61–85. https://doi.org/10.1016/j.apgeog.2005.09.001.

Al-Rowaily, S.L., El-Bana, M.I., Al-Dujain, F.A.R., 2012. Changes in vegetation composition and diversity in relation to morphometry, soil and grazing on a hyper-arid watershed in the central Saudi Arabia. CATENA 97, 41–49. https://doi.org/10.1016/j.catena.2012.05.004.

Arshad, M., Alrumman, S.A., Eid, E.M., 2018. Evaluation of carbon sequestration in the sediment of polluted and non-polluted locations of mangroves. Fund. Appl. Limnol. 192, 53–64. https://doi.org/10.1127/fal/2018/1127.

Batisani, N., Yarnal, B., 2009. Urban expansion in Centre County, Pennsylvania: Spatial dynamics and landscape transformations. Appl. Geogr. 29, 235–249. https://doi.org/10.1016/j.apgeog.2008.08.007.

Briem, G.J., Benediktsson, J.A., Sveinsson, J.R., 2002. Multiple classifiers applied to multisource remote sensing data. IEEE T. Geosci. Remote Sens. 40, 2291–2299. https://doi.org/10.1109/TGRS.2002.802476.

Chaudhary, H., 1999–2001. Flora of Kingdom of Saudi Arabia vol. I, II and III. Ministry of Agriculture and Water, National Herbarium, National and Water Research Center, Riyadh, Saudi Arabia.

Chavez, P., Berlin, G.L., Sowers, L.B., 1982. Statistical method for selecting landsat MSS. J. Appl. Photogr. Eng. 8, 23–30.

Chen, X., Vierling, L., Deering, D., 2005. A simple and effective radiometric correction method to improve landscape change detection across sensors and across time. Remote Sens. Environ. 98, 63–79. https://doi.org/10.1016/j.rse.2005.05.021.

Cohen, J., 1960. A coefficient of agreement for nominal scales. Educ. Psychol. Meas. 20, 37–46. https://doi.org/10.1177/001316446002000104.

Congalton, R., Mead, R., 1983. A quantitative method to test for consistency and correctness in photointerpretation. Photogramm. Eng. Remote Sens. 49, 69–74.

Congalton, R.G., 1991. A review of assessing the accuracy of classifications of remotely sensed data. Remote Sens. Environ. 37, 35–46. https://doi.org/10.1016/0034-4257(91)90048-B.

Coppin, P., Jonckheere, I., Nackaerts, K., Muys, B., Lambin, E., 2004. Digital change detection methods in ecosystem monitoring: a review. Int. J. Remote Sens. 25, 1565–1596. https://doi.org/10.1080/0143116031000101675.

Dewan, A.M., Yamaguchi, Y., 2008. Using remote sensing and GIS to detect and monitor land use and land cover change in Dhaka Metropolitan of Bangladesh during 1960–2005. Environ. Monit. Assess. 150, 237. https://doi.org/10.1007/s10661-008-0226-5.

El-Sheikh, M.A., Al-Shehri, M.A., Alfarhan, A.H., Alatar, A.A., Rajakrishnan, R., Al-Rowaily, S.L., 2019. Threatened *Prunus arabica* in an ancient volcanic protected area of Saudi Arabia: Floristic diversity and plant associations. Saudi J. Biol. Sci. 26, 325–333. https://doi.org/10.1016/j.sjbs.2018.02.001.

Elhag, M., Bahrawi, J., 2014a. Cloud coverage disruption for groundwater recharge improvement using remote sensing techniques in Asir region, Saudi Arabia. Life Sci. J. 11, 192–200.

Elhag, M., Bahrawi, J., 2014b. Conservational use of remote sensing techniques for a novel rainwater harvesting in arid environment. Environ. Earth Sci. 72, 4995–5005. https://doi.org/10.1007/s12665-014-3367-6.

Elhag, M., Psilovikos, A., Sakellariou, M., 2013. Detection of land cover changes for water recourses management using remote sensing data over the Nile Delta Region. Environ. Dev. Sustain. 15, 1189–1204.

Gao, J., Liu, Y., 2010. Determination of land degradation causes in Tongyu County, Northeast China via land cover change detection. Intl. J. Appl. Earth Obs. Geoinfo. 12, 9–16. https://doi.org/10.1016/j.jag.2009.08.003.

Geymen, A., Baz, I., 2008. The potential of remote sensing for monitoring land cover changes and effects on physical geography in the area of Kayisdagi Mountain and its surroundings (Istanbul). Environ. Monit. Assess. 140, 33–42. https://doi.org/10.1007/s10661-007-9844-6.

Giri, C., Zhu, Z., Reed, B., 2005. A comparative analysis of the Global Land Cover 2000 and MODIS land cover data sets. Remote Sens. Environ. 94, 123–132. https://doi.org/10.1016/j.rse.2004.09.005.

Green, D.R., 2011. Remote sensing with IDRISI Taiga: a beginner's guide, by Timothy A. Warner and David. J. Int. J. Remote Sens. 32, 7901–7902. https://doi.org/10.1080/01431161.2010.51672.

Hill, M.O., 1979a. DECORANA: A FORTRAN Program for Detrended Correspondence Analysis and Reciprocal Averaging. Section of Ecology and Systematics. Cornell University, NY.

Hill, M.O., 1979b. TWINSPAN: A FORTRAN Program for Arranging Multivariate Data in an Ordered Two-way Table by Classification of the Individuals and Attributes. Section of Ecology and Systematics. Cornell University, NY.

Hsu, C.-W., Chang, C.-C., Lin, C.-J., 2003. A Practical Guide to Support Vector Classification. National Taiwan University, Taiwan.

Huang, W., Liu, H., Luan, Q., Jiang, Q., Liu, J., Liu, H., 2008. Detection and prediction of land use change in Beijing based on remote sensing and GIS. Int. Arch. Photogramm. Remote Sens. Spat. Inf. Sci 37, 75–82.

Jensen, J.R., Rutchey, K., Koch, M.S., Narumalani, S., 1995. Inland wetland change detection in the Everglades Water Conservation Area 2A using a time series of normalized remotely sensed data. Photogramm. Eng. Remote Sens. 61, 199–209.

Jiao, F., Wen, Z.-M., An, S.-S., 2011. Changes in soil properties across a chronosequence of vegetation restoration on the Loess Plateau of China. CATENA 86, 110–116. https://doi.org/10.1016/j.catena.2011.03.001.

Kassas, M., Imam, M., 1954. Habitat and plant communities in the Egyptian Desert: III. The Wadi bed ecosystem. J. Ecol. 42, 424–441. https://doi.org/10.2307/2256869.

Kent, M., 2012. Vegetation Description and Data Analysis: A Practical Approach. John Wiley & Sons, Chichester.

Kloer, B., 1994. Hybrid parametric/non-parametric image classification. ACSM-ASPRS Annual Convention, 15, pp. 307–316.

Kumar, A., Khan, M.A., Muqtadir, A., 2010. Distribution of mangroves along the Red Sea coast of the Arabian Peninsula: Part-I: the northern coast of western Saudi Arabia. Earth Sci. India 3, 28–42.

Lu, D., Mausel, P., Brondízio, E., Moran, E., 2004. Change detection techniques. Int. J. Remote Sens. 25, 2365–2401. https://doi.org/10.1080/0143116031000139863.

Mahmoud, A., El-Sheikh, A., Isawi, F., 1982. Ecology of the littoral salt marsh vegetation at Rabigh on the Red Sea coast of Saudi Arabia. J. Arid Environ. 5, 35–42. https://doi.org/10.1016/S0140-1963(18)31461-7.

Mas, J.F., 1999. Monitoring land-cover changes: A comparison of change detection techniques. Int. J. Remote Sens. 20, 139–152. https://doi.org/10.1080/014311699213659.

Pelorosso, R., Leone, A., Boccia, L., 2009. Land cover and land use change in the Italian central Apennines: A comparison of assessment methods. Appl. Geogr. 29, 35–48. https://doi.org/10.1016/j.apgeog.2008.07.003.

Richards, J.A., Richards, J., 1999. Remote Sensing Digital Image Analysis. Springer-Verlag, Berlin.

Rivera, V.O., 2005. Hyperspectral Change Detection Using Temporal Principal Component Analysis. University Of Puerto Rico, Spain.

Shalaby, A., Tateishi, R., 2007. Remote sensing and GIS for mapping and monitoring land cover and land-use changes in the Northwestern coastal zone of Egypt. Appl. Geogr. 27, 28–41. https://doi.org/10.1016/j.apgeog.2006.09.004.

Singh, A., 1989. Digital change detection techniques using remotely-sensed data. Int. J. Remote Sens. 10, 989–1003. https://doi.org/10.1080/01431168908903939.

Swain, P.H., Davis, S.M., 1981. Remote sensing: the quantitative approach. IEEE Trans. Pattern Anal. Mach. Intell., 713–714

Vesey-Fitzgerald, D.F., 1957. The vegetation of the Red Sea coast, north of Jeddah, Saudi Arabia. J. Ecol. 45, 547–562.

Wang, F., Xu, Y.J., 2010. Comparison of remote sensing change detection techniques for assessing hurricane damage to forests. Environ. Monit. Assess. 162, 311–326. https://doi.org/10.1007/s10661-009-0798-8.

Whitford, W.G., 2002. Ecology of Desert Systems. Elsevier, New York.

Yuan, D., Elvidge, C.D., Lunetta, R.S., 1998. Survey of multispectral methods for land cover change analysis. In: Lunetta, R.S., Elvidge, C.D. (Eds.), Remote Sensing Change Detection: Environmental Monitoring Methods and Applications. Ann Arbor Press, Chelsea, MI, pp. 21–39.

Yuan, F., Sawaya, K.E., Loeffelholz, B.C., Bauer, M.E., 2005. Land cover classification and change analysis of the Twin Cities (Minnesota) Metropolitan Area by multitemporal Landsat remote sensing. Remote Sens. Environ. 98, 317–328. https://doi.org/10.1016/j.rse.2005.08.006.

Zhou, W., Troy, A., Grove, M., 2008. Object-based land cover classification and change analysis in the Baltimore metropolitan area using multitemporal high resolution remote sensing data. Sensors 8, 1613. https://doi.org/10.3390/s8031613.